Utilizing Data Mining to Develop a Model to Predict Individuals at Elevated Risk for Anterior Cruciate Ligament Injury

[1]Kristin D. Morgan, [2]Cyril J. Donnelly, and Jeffrey A. Reinbolt[1]
[1]University of Tennessee, 1512 Middle Drive, Knoxville, TN 37996-2210
[2]The University of Western Australia, Perth, Western Australia, Australia

Abstract

The purpose of this study is to utilize data mining to discern hidden patterns in the joint biomechanics and electromyography (EMG) data of individuals at risk for Anterior Cruciate Ligament (ACL) injury. While it is important to know which biomechanical factors contribute to movement, it is also critical to determine how they function differently in individuals at high and low risk for ACL injury. In this study a large dataset of experimental kinetic and EMG data was used to determine relationships among these biomechanical variables and ACL injury risk. We assess this relationship using functional data analysis techniques that utilize statistical methods, such as principal component analysis (PCA), to isolate such relationships. The end goal is to use the resulting models to identify individuals at high risk for ACL injury.

Keywords: Data Mining, Principal Component Analysis, Wavelets, Order Recurrence Plots, Predictive Modeling, Anterior cruciate ligament injury

1. Introduction

Statistical analysis and data mining techniques may provide one avenue to identify available neuromuscular countermeasures to reduce an athlete's risk of ACL injury. In general, researchers have the capacity to collect and calculate a significant amount of data from a cadre of measurement devices and computational modeling tools. Yet, not every piece of data is meaningful or essential to answering a given research question [1]. The key is to extract or "mine" the relevant features within these large, multivariate datasets [1]. Traditionally, researchers in the ACL injury prevention field record discrete measurements, such as mean knee flexion angle at impact and knee flexion range of motion following impact [2, 3]. Peak abduction knee angle and knee abduction moments within the impact phase (20-30%) of stance [4] are also analyzed to make clinical assessments of human movement. However, additional information can be gained by analyzing biomechanical waveforms, such as joint motion and muscle activations over time, to capture the variability in muscle recruitment strategies and/or human movement performance. Thus, principal component analysis (PCA) and wavelet analysis will be employed to detect movement abnormalities in large biomechanical datasets.

Principal component analysis (PCA) is a valuable tool in detecting variability in human movement [1, 5, 6]. PCA is a statistical technique that reduces large, high-dimensional datasets to a smaller subset of orthogonal vectors called principal components. From these components it is possible to detect the dominant features and sources of variability within the waveform data. It has been successful in clinical applications to 1) aid the identification of differences in lifting kinematics and kinetics between healthy individuals and populations with lower back pain, 2) distinguish between the frontal plane kinetics of male and female subjects during unanticipated cutting maneuvers, and 3) assess the success of two total hip arthroplasty surgical approaches in restoring the normal gait patterns post-surgery [7-9]. The success of PCA in the aforementioned clinical applications provides precedent for its use in identifying specific muscle recruitment strategies distinct to populations classified as low and high risk of ACL injury.

Wavelet analysis can also be used to detect anomalies in time series. This approach involves reducing the original waveform into wavelets, shortened versions of the original waveform to identify and analyze patterns and/or abnormalities in the data [10]. With respect to the human body, wavelets have been used to analyze brain activity, heart rhythms, the onset of seizures, myocardial infarctions and to detect hidden features and/or elements within the genetic code. However, its application in human movement is lesser known [11-13]. This study will use this technique to analyze muscle activity derived from electromyography (EMG) data with the aim of detecting abnormalities associated with at-risk individuals.

Wavelet analysis is a preferred method of time series analysis over alternative techniques; such as, Fourier analysis and autoregressive integrated moving average (ARIMA) models, because wavelets preserve both the spatial and temporal components of the original signal, whereas in the case of the Fourier analysis only the frequency component is retained [10]. There are a multitude of wavelet analysis techniques that can be applied; however, this study will use one of the simplest [14]. The Haar wavelet is a discrete waveform transform that divides the signal into a trend and fluctuation. Each of these signals is half the length of the original signal thus resulting in multiple cycles of calculating trends and fluctuations that can be analyzed to detect abnormalities hidden in these various sub-signals. While the temporal plots of the trend and fluctuation data will be examined to identify abnormalities, an additional technique - Order Recurrence Plots (ORPs) - will be used as a method for visually observing the anomalies in the data captured by the Haar wavelet analysis. ORPs are used to analyze dynamic systems where the focus is to distinguish between ordered patterns or chaos in the data or to determine the point of transition between ordered and chaotic behavior [15]. Utilizing ORPs in combination with Haar wavelets will allow us to further determine if there are any patterns in the Haar trend and difference data that can be associated with injury risk. In this study, Haar wavelet analysis and ORPs will be used to explore EMG data for muscle activity abnormalities in the six muscles surrounding the knee.

PCA will also be used in conjunction with this wavelet analysis to detect unique features that earmark at-risk individuals prone to ACL injuries. First, PCA will be used to correlate changes in knee kinematics and kinetics to muscle function via EMG data during a single-leg jump landing task (Figure 1). Next, wavelet analysis will be used to extract hidden patterns in EMG data and map them to the PCA result. It is our view that such an approach can be quite fruitful.
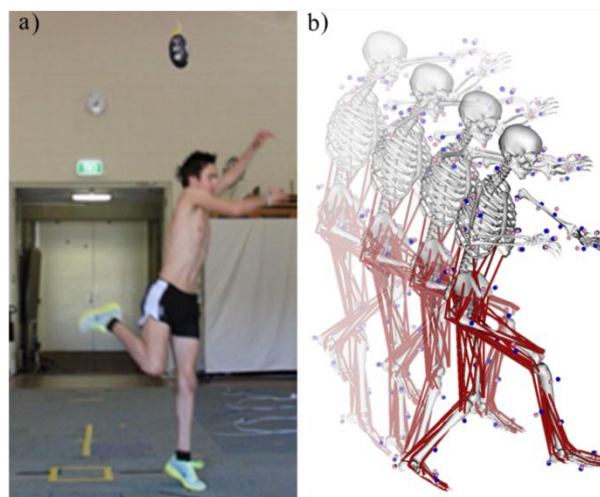
Figure 1. (a) Subject performing the experimental single-leg jump landing protocol in the laboratory. (b) Simulation of single-leg jump landing task using a model with 37 degrees-of-freedom and driven by 92 muscle-tendon actuators.

2. Methodology

2.1 Analytical Techniques

2.1.1. Principal Component Analysis

PCA was used to identify waveform variability from the joint kinetic data for all subjects during the weight acceptance (WA) phase of single-leg jump landing. To perform the analysis, matrices were created where the time during the WA phase of landing consists of 101 data points contained in seven kinetic variable columns (n = 7). Two trials were conducted for each of seven subjects. Thus the total experimental sample space was represented by seven matrices that included the sagittal, frontal and transverse plane hip, knee and ankle kinetics for the 14 trials that the subjects performed.

PCA is a multistep process. For each variable of interest in the study, the first step involved subtracting the mean from each observation. Next, the covariance matrix was used to calculate the eigenvalue-eigenvector pairs that represented the principal components (PC) loadings and principal components (PCs), respectively. The PCs were placed in order from highest to lowest based on their associated loadings. PC 1 was the PC with the largest associated loading that accounted for the greatest percentage of variance in the data. The set of PCs that explained at least 90% of the variance were used for further analysis. The 90% criteria was used instead of the Cattell and Kaiser criteria, since the latter usually over or under estimates component levels needed to appropriately explain waveform variance [16]. From the PC loadings and PCs, PC scores are generated that represent the data in the new rotated space [16]. For this study the variable of interest was the knee abduction moment. This variable was selected because the elevated knee abduction moment during landing has been found to increase ACL strain in cadaveric knee models [17] and predicts ACL injury rates [18]. The PC loadings for the knee abduction moment will be utilized to determine a relationship between joint biomechanics waveform variability and muscle activation and to identify differences in muscle activation strategies used by subjects at varying risk of ACL injury during the single-leg jump landing. All of the aforementioned analyses were performed using Matlab for Windows (Matlab R2012a, The Math Works, Natick, Massachusetts, USA).

2.1.2. Wavelet Analysis

Fourteen EMG data trials were collected from the pool of athletes for the analysis. EMG waveforms for six of the muscles that cross the knee - the vastus medialis, vastus lateralis, medial and lateral hamstrings and medial and lateral gastrocnemii - were analyzed during the WA phase of landing. Haar wavelet analysis was performed on each waveform individually calculating the trend and fluctuation signals. The trend signal is the average of successive data points from the (a) original waveform divided by square root of two (Eq. 1) [14].

$$a_1 = \frac{f_1 + f_2}{\overline{2}} \qquad (1)$$

The fluctuation (d) is the difference between successive data points again multiplied by the square root of two (Eq.2) [14].

$$d_1 = \frac{f_1 - f_2}{\overline{2}} \qquad (2)$$

Four reductions of the data yield four trends (a1-a4) and four fluctuation (d1-d4) wavelets for each muscle waveform. This analysis was conducted in Matlab (Matlab 7.8, The Math Works, Inc., Natick Massachusetts, USA).

ORPs were created for the unfiltered EMG data, the Haar trends (a1-a4) and fluctuations (d1-d4) data. The ORPs were constructed using the following threshold relationship (3)[15].

$$R_{i,j}(\varepsilon) = \Theta\left(\varepsilon - \left\|\vec{x}_i - \vec{x}_j\right\|\right), \quad i,j = 1, \dots, N, \quad (3)$$

N = number of measured points of $\vec{x}_i$
Θ = Heaviside function
ε = threshold or cut off distance
$\|\cdot\|$ = norm

$$R_{i,j}(\varepsilon) = \begin{cases} 1 : & \left\|\vec{x}_i - \vec{x}_j\right\| \le \varepsilon \\ 0 : & otherwise \end{cases} \quad \vec{x}_i \in R^d, \; i,j = 1, \dots, N, \quad (4)$$

Whenever the difference between the two signals $x_i - x_j$ falls within the boundary defined by ε, $R_{i,j}(\varepsilon)$ is assigned a value of one. However, if this difference lies outside of the boundary, it is assigned a value of 0 via Equation 4 [15]. In ORPs, the ones are represented by the color black and zeroes are in red. The ORPs were assessed visually to determine if they were symmetric along the main diagonal line. This was used to indicate whether similar muscles produced analogous jump landing movement. The symmetry observed in the plots will be quantified using the kendall tau rank correlation that measures the correlation between datasets (Equation 5) [19]. This analysis was also conducted in Matlab (Matlab 7.8, The Math Works, Inc., Natick Massachusetts, USA).

$$\tau = \frac{(numer\ of\ concordant\ pairs) - (numer\ of\ discordant\ pairs)}{\frac{1}{2}n(n-1)} \quad (5)$$

n = number of pairs

2.2 Experimental Protocol

Thirty-four Western Australian Amateur Football players were recruited to complete a single-leg jump landing protocol. Joint kinematics and ground reaction force (GRF) measurements were obtained from the experimental motion capture data collected during the protocol. For the single-leg jump landing protocol, subjects were instructed to jump from their preferred leg, and while in flight, an Australian football was randomly swung medially or laterally to the subjects approach direction [20]. The height of the ball was approximately 90% of each subject's maximal vertical jump height. After the subject had successfully grabbed the football in flight, they were instructed to contact the force platform with the same right leg from which they jumped. The single-leg jump landing trial where the Australian football was swung laterally or away from their stance leg was used for further analysis. Seven athletes (age 20.7 ± 1.8 years; mass 87.9 ± 5.1kg; height 1.87 ± 0.1m) were randomly selected from the cohort, which has been described previously [21]. All of the experimental procedures were approved by the University of Western Australia Human Research Ethics Committee and all subjects provided their informed written consent prior to data collection.

During the single-leg jump landing task, experimental kinematic marker trajectories, GRF, and surface electromyography (sEMG) data were collected from each subject. Three-dimensional, full-body kinematics were recorded using a12-camera, 250 Hz VICON MX motion capture system (VICON Peak, Oxford Metrics Ltd., UK) [22, 23]. The GRF data were synchronously recorded at 2,000 Hz using an AMTI (Advanced Mechanical Technology Inc., Watertown, MA) 1.2 x 1.2m force platform. Both the kinematic and GRF data were low-pass filtered at 20 Hz using a zero phase-shift 4th-order Butterworth

digital filter in Workstation (ViconPeak, Oxford Metrics Ltd., UK). Additionally, sEMG data were collected at 2,000 Hz for six muscles: vastus medialis, vastus lateralis, medial and lateral gastrocnemius and medial and lateral hamstrings.

Multiple three-dimensional 14-segment, 37 degree-of-freedom (DoF), 92 muscle-tendon actuated subject-specific models were created in OpenSim 1.9.1 to generate simulations of the subjects performing single-leg jump landings (Fig. 1) [24]. Each simulation was generated using a three-step process. First, the model's segment lengths and mass were scaled to each subject. Second, joint kinematics were calculated from experimental kinematic marker data using inverse kinematics (IK). Third, residual reduction analysis (RRA) was used to create dynamically consistent simulations with the experimentally recorded ground reaction forces [22]. These dynamically consistent simulations were analyzed during the weight-acceptance (WA) phase of single-leg jump landing. The WA phase of landing was analyzed since this is the period when knee abduction and internal rotation moments acting on the knee are the highest and it is assumed that the ligament is at the greatest risk of injury [22, 23].

3. Results

3.1 Principal Component Analysis

In the study, principal components analyses were conducted on the muscle moment measurement data captured for two experimental trials – Trial A and Trial B – for each of the fourteen participants. Principal component loadings for the knee abduction moment indicated that Trial B was a strong source of variability (loading = 0.40) whereas Trial A was a smaller value (loading = 0.05) given that Trial B fell above the 0.25 PC loading cutoff line (Figure 2). Furthermore, Trial B was a strong source for variability (loading = -0.42) and again Trial A was a smaller source of variability (Loading = -0.04) for knee internal rotation moment, while all subject trials showed similar loadings for knee flexion moment.
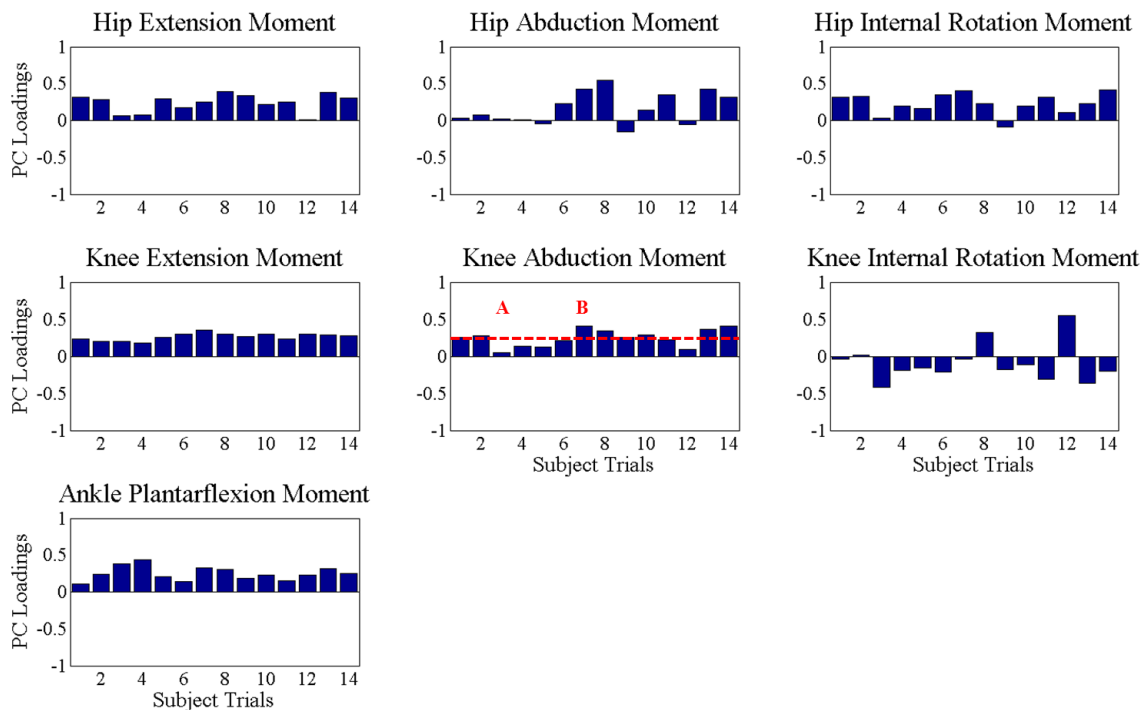
Figure 2. Principal component loadings for lower extremity joint biomechanics during single-leg jump landing task. The dotted red line represents the PC loading cutoff value of 0.25. Trials that fall above the line are designated at strong sources of variability while trials that fall below the line are designated as smaller sources of variability. The labels A and B represent trials that will be used for the subsequent analyses.

3.2 Wavelet Analysis

The preliminary Haar wavelet analysis of the vastus medialis EMG data for the individuals of Trials A and B revealed an interesting pattern. With Trial A (Figure 3) a significant spike precedes a smaller one while the converse holds for Trial B (Figure 4). Such cyclical patterns were also observed in the other muscles; however, none occurred for both subjects.
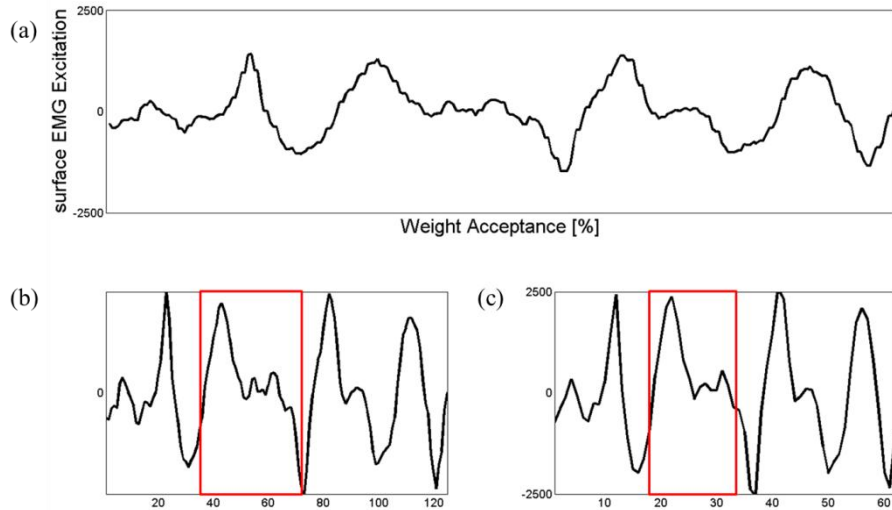
Figure 3. Comparison of unfiltered EMG data (a) and the first (b) and second (c) trends of Haar wavelet transformed EMG analyzed during the weight-acceptance phase of single-leg jump landing for Trial A.
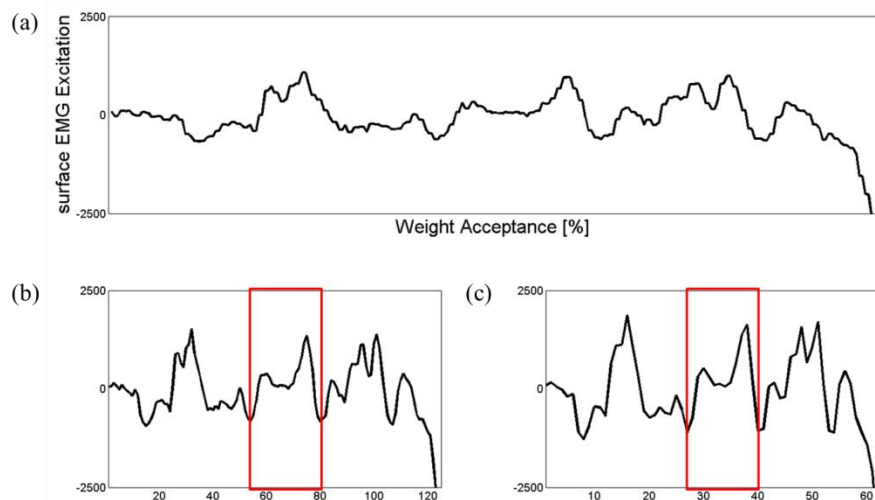
Figure 4. Comparison of unfiltered EMG data (a) and the first (b) and second (c) trends of Haar wavelet transformed EMG analyzed during the weight-acceptance phase of single-leg jump landing for Trial B.

Analysis of the companion ORPs likewise confirmed the presence of these cyclical patterns in the data as indicated by repeating checkerboards (Figures 3-4). The larger the structure and/or pattern the more ordered the data. However, the appearance of smaller more grain like patterns and structures indicate that the data are more chaotic. The vastus medialis and medial hamstring displayed a more ordered pattern than the vastus lateralis, lateral hamstring and gastrocnemii muscles for Trial A when plotted against themselves. All six muscles displayed similar, moderate-sized patterns for Trial B also when plotted against themselves. Yet, the plots for each muscle plotted against itself was symmetric about the diagonal

(bottom left corner to top right corner) to represent that the two signals exhibited the same pattern, which is expected when plotting a signal against itself.

The ORPs for Trial A and B provide a within muscle group analysis. Such plots of the medial and lateral quadriceps (vasti muscles), hamstrings and gastrocnemii muscles reveal that although functional similar muscles within the muscles groups do perform exactly the same, there are some asymmetries in the ORPs for both trials (Figures 5-6).

The kendall tau rank correlation was used to quantify this relationship between muscles noted in the ORPs (Tables 1 and 2). The kendall tau rank correlation verified the symmetric relationship when analyzing the muscles against themselves recording a value of 1 (perfect agreement between two datasets). The medial and lateral gastrocnemii muscles had the largest kendall tau value for the within muscle analysis at 0.35 revealing that those muscles were moderately correlated for Trial B, while the medial and lateral vasti also displayed a weaker, positive correlation of 0.28. However, the medial and hamstring muscles were weakly negatively correlated at -0.16. For Trial A, the quadriceps, hamstrings and gastrocnemii muscle groups were all negative, weakly correlated at -0.20, -0.19 and -0.15, respectively.
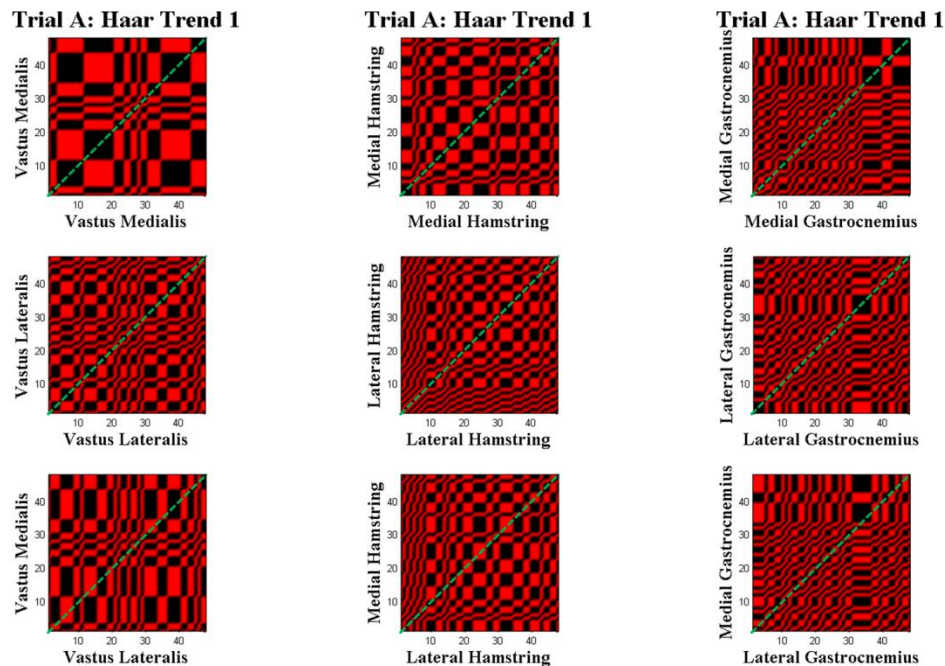
Figure 5. Order recurrence plots of the Haar 1 transform of the medial and lateral vasti, hamstring and gastrocnemii muscles for Trial A. The first two rows of ORPs are plots of the individual muscles plotted against themselves with the third row of the medial and lateral vasti, hamstring and gastrocnemii plotted against each other. The dotted green lines are utilized to assess the symmetry within the plot to evaluate the synchronization between two signals.
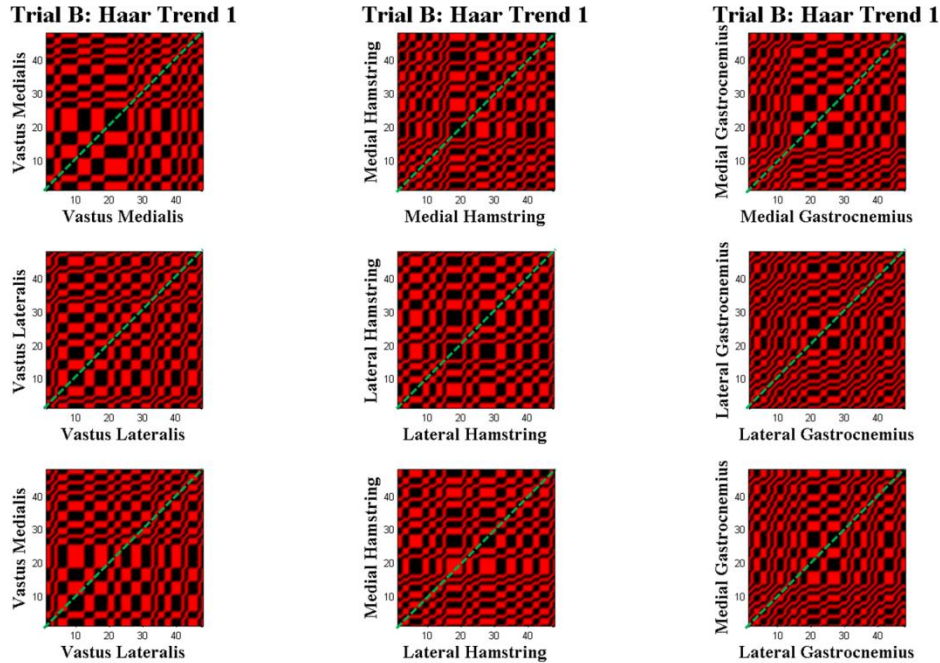
Figure 6. Order recurrence plots of the Haar 1 transform of the medial and lateral vasti, hamstring and gastrocnemii muscles for Trial B. The first two rows of ORPs are plots of the individual muscles plotted against themselves with the third row of the medial and lateral vasti, hamstring and gastrocnemii plotted against each other. The dotted green lines are utilized to assess the symmetry within the plot to evaluate the synchronization between two signals.

Table 1: Kendall tau rank correlation coefficients between the Haar 1 transform of the medial and lateral vasti, hamstrings and gastrocnemii muscle groups for Trial A.

Haar 1 Trend	Vastus Medialis	Vastus Lateralis	Medial Hamstring	Lateral Hamstring	Medial Gastrocnemius	Lateral Gastrocnemius
Vastus Medialis	1.00	-0.20	0.23	-0.22	0.17	0.20
Vastus Lateralis	-0.20	1.00	-0.32	0.25	0.10	-0.20
Medial Hamstring	0.23	-0.32	1.00	-0.19	0.13	0.16
Lateral Hamstring	-0.22	0.25	-0.19	1.00	0.11	-0.15
Medial Gastrocnemius	0.17	0.10	0.13	0.11	1.00	-0.15
Lateral Gastrocnemius	0.20	-0.20	0.16	-0.15	-0.15	1.00

Table 2: Kendall tau rank correlation coefficients between the Haar 1 transform of the medial and lateral vasti, hamstrings and gastrocnemii muscle groups for Trial B.

Haar 1 Trend	Vastus Medialis	Vastus Lateralis	Medial Hamstring	Lateral Hamstring	Medial Gastrocnemius	Lateral Gastrocnemius
Vastus Medialis	1.00	0.28	0.00	0.18	0.06	0.04
Vastus Lateralis	0.28	1.00	0.02	0.26	-0.07	-0.11
Medial Hamstring	0.00	0.02	1.00	-0.16	-0.29	0.31
Lateral Hamstring	0.18	0.26	-0.16	1.00	0.03	-0.09
Medial Gastrocnemius	0.06	-0.07	-0.29	0.03	1.00	0.35
Lateral Gastrocnemius	0.04	-0.11	0.32	-0.09	0.35	1.00

4. Discussion

These results demonstrate that the individuals in Trials A and B exhibited alternate knee abduction biomechanics during single-leg jump landing based on their knee abduction moment from the PC loading values. Utilizing wavelet analysis to investigate muscle function along with PCA enhances muscle function differences during landing. Muscle patterns of Trial A showed minimal correlation between the medial and lateral muscles for the quadriceps, hamstring and gastrocnemii muscles. Such patterns in Trial B showed a more moderate correlation particularly between the gastrocnemii muscles. A negative value for the medial and lateral muscles for Trial A indicated that those muscles were inversely correlated.

Anecdotally, ACL injuries are characterized by a medial collapse of the knee. Hence it is possible that at the muscular level there is an imbalance of the medial and lateral muscles that support the knee; such as, the quadriceps, hamstrings and gastrocnemii muscles. Equal activation and force production of the medial and lateral muscles may be the key to resisting the medial collapse of the knee, maintaining joint stability and potentially reducing ACL injury risk. Together the ORPs and kendall tau rank correlation both visually and quantitatively, detected the muscle function of individuals during landing. While neither individual displayed strong correlation between the medial and lateral quadriceps, hamstrings and gastrocnemii muscles, the moderately strong relationships between the gastrocnemii muscles and even the quadriceps muscles could indicate a reduced risk of ACL injury for the individual in Trial B based on moderate medial and lateral muscle balance and/or symmetry.

The individual in Trial B was identified as the dominant source of variability in the group, which upon initial analysis via PCA, indicated that this individual was at an elevated risk of injury compared to the other individuals due to their differing knee abduction waveform biomechanics. However, further analysis uncovered that this individual actually exhibited moderate medial and lateral muscle symmetry, which would suggest reduced ACL injury risk. PCA is a technique that is used to identify the source of variability within a dataset; however, it is up to the researcher to determine how to interpret the results. In this study, it was easy to quickly classify the individual responsible for Trial B, which was identified as the source of variability, as an individual at elevated risk for ACL injury; yet, additional analysis

indicated the opposite. While this individual was displaying alternate knee biomechanics, their biomechanics were potentially the biomechanics of an individual at low-risk for injury, within a dataset of individuals that were at high-risk of injury, which would make their waveform stand out. This highlights why researchers need to be careful when interpreting their data and why it is useful to employ multiple techniques to validate their interpretations.

Future work will involve analyzing the additional 20 kinematic, kinetics and EMG trials to determine if the trends here are evident for all individuals. Additionally, alternate wavelet analysis techniques, including Daubechies and Continuous Wavelet Transform (CWT), will be explored to determine if they can provide added insight into varying muscle function via EMG waveform analysis. However, the results from this study indicate the potential of data mining techniques, such as PCA and wavelet analysis, to identify individuals at high risk for ACL injury.

Acknowledgements

References

[1]   Donnelly, C.J., et al., *An anterior cruciate ligament injury prevention framework: incorporating the recent evidence.* Res Sports Med, 2012. **20**(3-4): p. 239-62.

[2]   Lyman, S., et al., *Epidemiology of anterior cruciate ligament reconstruction: trends, readmissions, and subsequent knee surgery.* J Bone Joint Surg Am, 2009. **91**(10): p. 2321-8.

[3]   Daffertshofer, A., et al., *PCA in studying coordination and variability: a tutorial.* Clin Biomech (Bristol, Avon), 2004. **19**(4): p. 415-28.

[4]   Hashemi, J., et al., *Increasing pre-activation of the quadriceps muscle protects the anterior cruciate ligament during the landing phase of a jump: an in vitro simulation.* Knee, 2010. **17**(3): p. 235-41.

[5]   Hewett, T.E., et al., *Biomechanical measures of neuromuscular control and valgus loading of the knee predict anterior cruciate ligament injury risk in female athletes: a prospective study.* Am J Sports Med, 2005. **33**(4): p. 492-501.

[6]   Collins, J.J., C.C. Chow, and T.T. Imhoff, *Stochastic resonance without tuning.* Nature, 1995. **376**(6537): p. 236-238.

[7]   Priplata, A., et al., *Noise-Enhanced Human Balance Control.* Physical Review Letters, 2002. **89**(23).

[8]   Wrigley, A.T., et al., *Principal component analysis of lifting waveforms.* Clin Biomech (Bristol, Avon), 2006. **21**(6): p. 567-78.

[9]   O'Connor, K.M. and M.C. Bottum, *Differences in cutting knee mechanics based on principal components analysis.* Med Sci Sports Exerc, 2009. **41**(4): p. 867-78.

[10]   Dillard, B., *Hey, who turned off the lights?*, in *Chance*2010, Springer: 2010. p. 28-37.

[11]   Thomasson, N., et al., *Recurrence quantification in epileptic EEGs.* Physics Letters A, 2001. **279**: p. 94-101.

[12]   Chua, T., *A review of analytical techniques for gait data. Part 2: neural network and wavelet methods.* Gait and Posture, 2001. **31**: p. 102-120.

[13] Magdy, A., et al., *The Haar Wavelet Transform of the DNA Signal Representation.* World Academy of Science, Engineering and Technology, 2013. **73**: p. 667-673.

[14] Walker, J.S., *A primer on wavelets and their scientific applications*. 2008: CRC Press.

[15] Marwan, N., et al., *Recurrence plots for the analysis of complex systems.* Physics Reports, 2007. **438**(5-6): p. 237-329.

[16] Jolliffe, I.T., 2002. Principal Component Analysis, 2nd Ed Springer, New York.

[17] Marklof, K.L., Burchfield, D. M., Shapiro, M. M., Shepard, M. F., Finerman, G.A.M., and Slauterbeck, J.L., 1995. Combined knee loading states that generate high anterior cruciate ligament forces. *Journal of Orthopaedic Research* 13(6), 930-5.

[18] Hewett, T. E., Myer, G. D., Ford, K. R., Heidt, R. S., Jr., Colosimo, A. J., McLean, S. G., van den Bogert, A. J., Paterno, M. V. and Succop, P., 2005. Biomechanical measures of neuromuscular control and valgus loading of the knee predict anterior cruciate ligament injury risk in female athletes: A prospective study. *The American Journal of Sports Medicine* 33(4), 492–501.

[19] Nelsen, R.B., 2001. *Encyclopedia of Mathematics: Kendall tau metric*. 2001: Springer.

[20] Dempsey, A.R., Elliott, B.C., Munro, B.J. Steele, J.R. and Lloyd, D.G., 2012. Whole body kinematics and knee moments that occur during an overhead catch and landing task in sport. *Clinical Biomechanics* 27, 466-74.

[21] Donnelly, C.J., Elliott, B.C., Doyle, T.L.A., Finch, C.F., Dempsey, A.R. and Lloyd, D.G., 2012. Changes in knee joint biomechanics following balance and technique training and a season of Australian football. British *Journal of Sports Medicine* **46**, 917-22.

[22] Donnelly, C.J., Lloyd, D.G., Elliott, B.C. and Reinbolt, J.A., 2012. Optimizing whole-body kinematics to minimize valgus knee loading during sidestepping: implications for ACL injury risk. *Journal of Biomechanics* **45**, 1491-97.

[23] Dempsey, A.R., Lloyd, D.G., Elliott, B.C., Steele, J.R., Munro, B.J. and Russo, K.A., 2007. The effect of technique change on knee loads during sidestep cutting. *Medicine & Science in Sports & Exercise* **39**(10), 1765-73.

[24] Delp, S.L., Anderson, F.C., Arnold, A.S., Loan, P., Habib, A., John, C.T., Guendelman, E. and Thelen, D.G., 2007. OpenSim: open-source software to create and analyze dynamic simulations of movement. *IEEE Transactions on Biomedical Engineering* **54**, 1940-50.